



STRUCTURAL PERFORMANCE OF SEISMICALLY ISOLATED AND FIBER-REINFORCED CONCRETE BRIDGES

A. Aviram¹, K. R. Mackie², and B. Stojadinovic³

ABSTRACT

An analytical study was carried out to assess the improved seismic performance of typical reinforced concrete bridges in California by utilizing two performance-enhancement techniques. The technologies considered were lead rubber bearing isolators located underneath the superstructure and fiber-reinforced concrete for the construction of the bridge piers. Seismic performance was measured in terms of different engineering demand parameters on major bridge components in addition to traditional force and displacement demands. A typical five-span, single column-bent reinforced concrete bridge was redesigned using the two performance enhancement techniques and modeled in the OpenSees structural analysis package. Two alternative designs of the isolated bridge were analyzed, one with elastic column behavior and the other with minor inelastic column behavior (maximum displacement ductility demand of 2). Special reinforcement details were used for the plastic hinge zone of the fiber-reinforced concrete columns, previously tested in a separate experimental study. Pushover and nonlinear time history analyses using 140 ground motions were carried out for the different bridge systems. The static and dynamic analysis results demonstrate the effectiveness of bridge isolation in significantly reducing the displacement and force demand on the bridge piers. The use of fiber-reinforced concrete in the construction of bridge columns results in increased damage-tolerance, shear strength, and energy dissipation under cyclic loading of these structural members. The cost-effectiveness of these two performance enhancement strategies is demonstrated in a companion paper.

Introduction

Deficient structural design of precast and cast-in-place reinforced concrete infrastructure systems has resulted in significant damage or collapse of structures with older design details during previous global earthquakes (1971 San Fernando, USA; 1989 Loma Prieta, USA; 1994 Northridge, USA; 1995 Kobe, Japan; 1999 Kocaeli, Turkey; 1999 Chi-Chi, Taiwan, etc.). Efforts to increase the ductility capacity of reinforced concrete bridges through better detailing and

¹Ph.D. Candidate, Dept. of Civil and Environmental Eng., University of California, Berkeley CA 94720-1710

²Assistant Professor, Dept. of Civil and Environ. Eng., University of Central Florida, Orlando, FL 32816-2450

³Professor, Dept. of Civil and Environmental Eng., University of California, Berkeley CA 94720-1710

confinement have resulted in modern bridges that are more damage tolerant and less susceptible to collapse. Research efforts in recent years have focused on improving performance even further, particularly for sites with high seismicity or directivity effects, through performance enhancing devices, supplemental damping devices, and energy-dissipation mechanisms (Buckle *et al.* 2006; Lee *et al.* 2007). These technologies limit the displacement and load demand on the column bents, as well as improve their damage-tolerance characteristics. Among the performance enhancement and damage mitigation strategies proposed and tested for the new construction of bridge systems are the use of fiber-reinforced concrete (FRC) for the construction of bridge piers, the installation of base isolation devices underneath the superstructure, and the post-tensioning of bridge piers. The use of confining jacketing layers around the perimeter of bridge piers and restrainer cables have also been widely tested for the retrofit of damaged bridges.

The use of fiber-reinforced concrete for the construction of bridge piers, leading to increased load-carrying capacity, ductile post-peak response, and high damage-tolerance, was experimentally investigated in recent studies (Billington and Yoon 2004; Saiidi *et al.* 2009; Aoude *et al.* 2009). To the author's knowledge, no analytical or experimental studies have been carried out on bridge piers or bridge systems constructed using high-performance fiber-reinforced concrete that exhibits strain hardening tensile behavior with distributed cracking. Most of the studies focusing on the use of FRC materials for seismic applications carried out to date have been limited to buildings and building components (Filiatrault *et al.* 1995; Naaman *et al.* 2007). The effectiveness of different isolation devices and systems located underneath the superstructure of a bridge structure in uncoupling the substructure from the horizontal components of ground motion excitation and therefore reducing its displacement and force demand has been thoroughly assessed through numerous experimental and analytical research studies (Mosqueda *et al.* 2004; Grant *et al.* 2004; Warn and Whittaker 2006).

The evaluation of the seismic performance of isolated bridges using lead-rubber bearings and high-performance fiber-reinforced concrete bridge, in comparison to a fixed-base conventionally reinforced concrete bridge, is the main focus of this study. The assessment is carried out in terms of the force and displacement demand vs. capacity of the bridges, as well as other engineering demand parameters recorded for major structural bridge components. Two alternative designs of the isolated bridge are analyzed, one with elastic column behavior and the other with minor inelastic column behavior. This evaluation is performed by comparing modal, nonlinear static, and nonlinear time history analyses results obtained for three-dimensional bridge models. The cost-effectiveness resulting from the use of these performance enhancement techniques is presented in a companion paper.

Bridge Modeling

The following section summarizes the general design scheme, basic assumptions, final dimensions, and material properties used for the three-dimensional nonlinear models of the conventionally-reinforced concrete (RC), fiber-reinforced concrete (FRC), and seismically isolated (BI) bridge models implemented in the OpenSees structural analysis program (Mckenna *et al.* 2000). The modeling and analysis of the different bridge models was carried out in accordance with the recommendations by Aviram *et al.* (2008a, 2008b).

Benchmark RC Bridge

The RC bridge consists of an Ordinary Nonstandard reinforced concrete bridge with box-girder superstructure, typical column bent details, and simple geometric regularity (symmetry, zero skew, and uniform column height), designed according to AASHTO Standard Specifications for Highway Bridges (AASHTO 1996) and Caltrans Seismic Design Provisions (Caltrans 2004). The geometry of the RC bridge corresponding to Tested bridge type 1A by Ketchum *et al.* (2004) is presented in Figure 1.

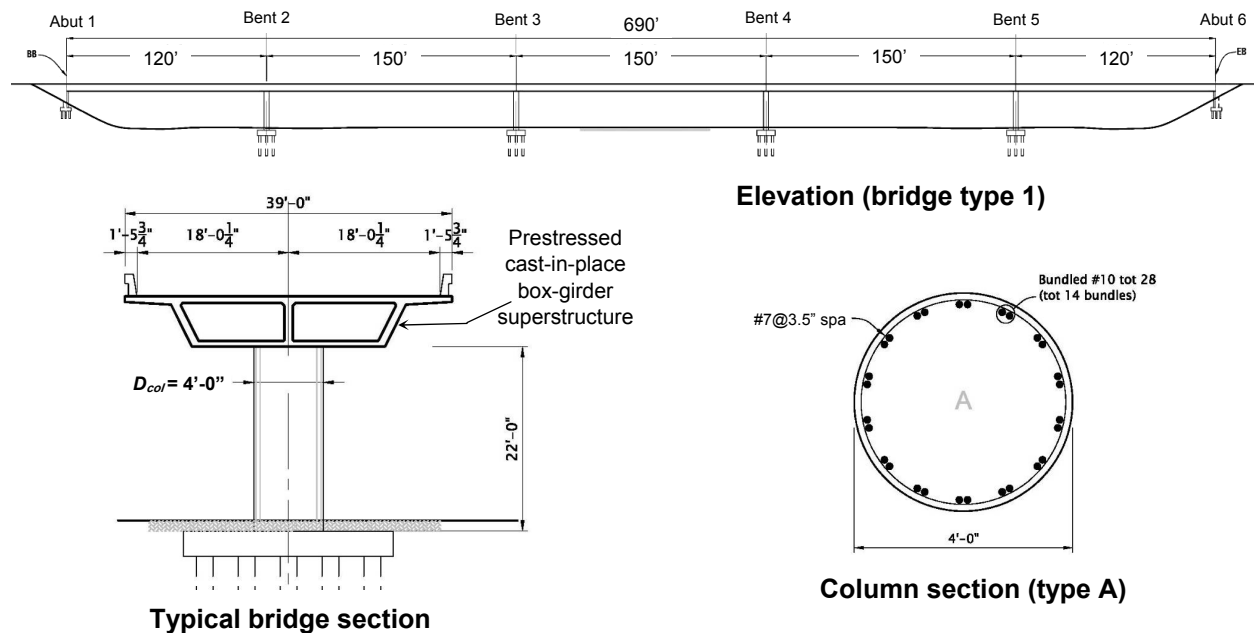


Figure 1. Geometry of the RC bridge type 1A (Ketchum *et al.* 2004).

The RC bridge superstructure was modeled using elastic beam-column elements and effective cross-section properties. The OpenSees model of the column bent consisted of a single segment with distributed plasticity fiber model, nonlinear force formulation and five integration points. Expected material strength properties were used for all steel and concrete elements and fibers, according to Caltrans SDC (2004). The concrete constitutive model used in OpenSees was *Concrete02* which has Kent-Scott-Park behavior and includes tensile strength. The steel fibers utilized *Steel02* which has Giuffre-Menegotto-Pinto behavior with ultimate strains specified according to Caltrans SDC (2004) and softening post-yield behavior. Rigid offsets were defined at the top of the column element to account for the column-superstructure moment connection. Lumped translational and rotational tributary mass were assigned to each node of the substructure and superstructure. The self-weight of the bridge and P-Delta effects were considered in the static and dynamic analysis. The column foundations were modeled as fixed boundary conditions and an elaborate abutment model developed by Mackie and Stojadinovic (2006), denoted as the Spring Abutment model, was used for the deck ends. This abutment model includes sophisticated longitudinal, transverse, and vertical nonlinear abutment response, as well as a participating mass corresponding to the concrete abutment and mobilized embankment soil.

FRC Bridge

The FRC bridge model in OpenSees was defined using the same geometry, superstructure, and abutment models as the RC bridge, and a modified column model specified according to the experimental results and analytical validation of FRC cantilever columns tested by Aviram *et al.* (2009). The tested FRC columns, constructed with steel macrofibers in 1.5% volume fraction, relaxed transverse reinforcement, additional dowel reinforcement at the column base, and unbonded region in the plastic hinge zone, presented improved cyclic behavior in comparison with the geometrically identical conventionally-reinforced concrete columns. Confined concrete behavior was defined for the fibers of both the core and cover of the FRC column cross section, according to FRC cylinder test results by Aviram *et al.* (2009). To account for the special reinforcement detailing at the base and plastic hinge zone, the total height of the column was divided into three segments, modeled as seen in Figure 2.

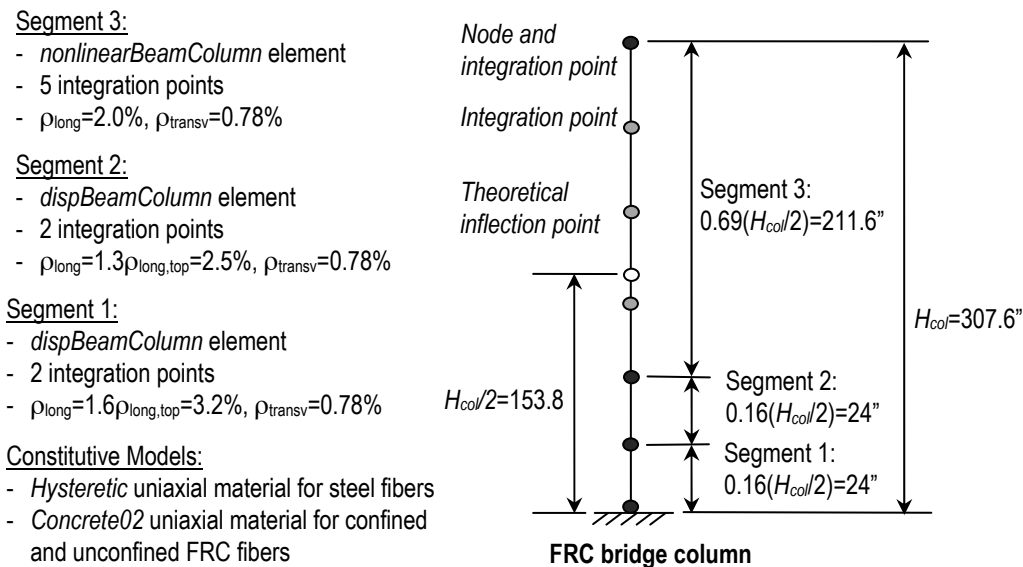


Figure 2. General scheme of the FRC bridge column model in OpenSees.

Isolated Bridges

The design of the isolated bridges was carried out for two target performance criteria: one with elastic column behavior (BI1) and the other with minor inelastic column behavior (maximum displacement ductility demand of 2) (BI2). The isolation devices selected for this bridge design to be placed underneath the superstructure consist of lead-plug rubber bearings (LRBs) with idealized bilinear behavior, commonly used for bridge isolation in North America. The LRB isolators were modeled in OpenSees using the *elastomericBearing* element developed and implemented for this study with bilinear response and circular interaction in shear. The axial, rotational, and torsional stiffnesses were approximated following the recommendations by Kelly (1997). Figure 3 presents the general modeling scheme used for the isolated bridges in OpenSees.

The abutment model implemented for the isolated bridges in OpenSees, denoted as the Isolator Abutment model was similar to the Spring Abutment model used for the RC bridge. The

uncoupled elastomeric bearings were replaced by the *elastomericBearing* element in OpenSees. To allow lateral displacement of the deck, the size of the longitudinal gap was increased and an additional compression-only gap was provided in the transverse direction, defined according to the maximum lateral displacement specified for the isolators (D_{max}). The shear keys and embankment mobilization in the transverse direction interacts with the superstructure and contributes to the shear resistance following gap closure.

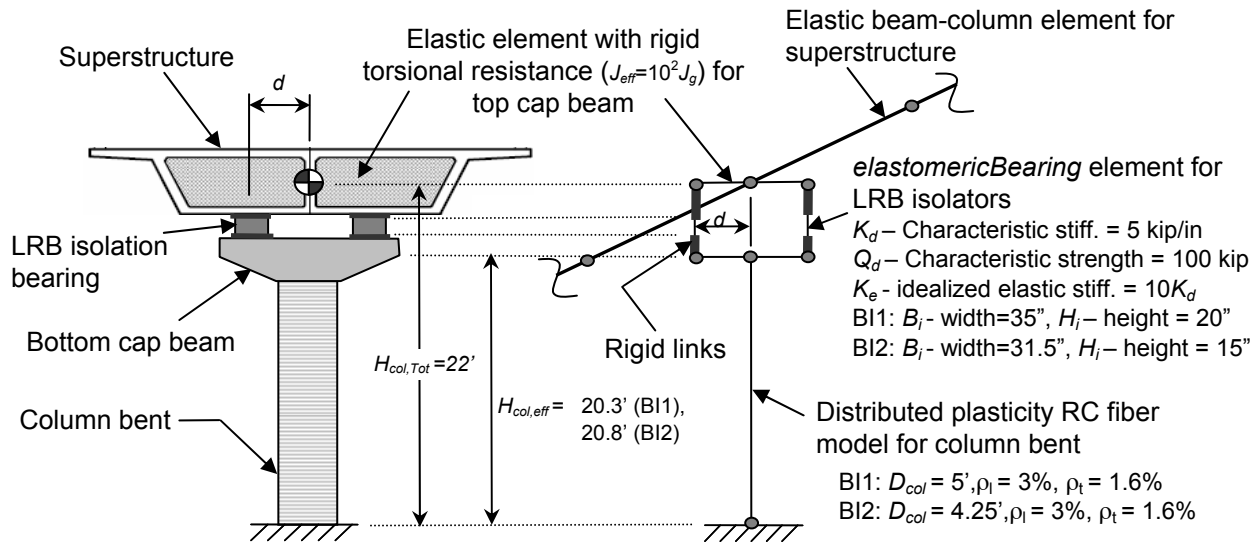


Figure 3. Schematic configuration of the isolated bridge models in OpenSees.

Modal Analysis Results

The modal periods of the nonlinear bridge models in OpenSees are presented in Table 1. The modal periods were obtained for the initial state of each nonlinear time history analysis where the column is uncracked (pre-earthquake period) and for the final state of each record, where column cracking and nonlinear behavior develops according to the ground motion characteristics and intensity (post-earthquake period). The post-earthquake modal periods in Table 1 were obtained for the El Centro Imp. Co. Cent. (B-ICC) record from the 1987 Superstition Hills earthquake with combined peak ground velocity (PGV) of 123.56 cm/sec (48.65 in/sec), representing a relatively high intensity ground motion.

Table 1. Pre- and post-earthquake (B-ICC record) periods of bridge models in OpenSees

Mode	RC bridge		FRC bridge		B11 bridge		B12 bridge	
	Pre-EQ	Post-EQ	Pre-EQ	Post-EQ	Pre-EQ	Post-EQ	Pre-EQ	Post-EQ
Transverse translation	0.95	1.15	1.01	1.35	1.42	1.66	1.51	1.55
Longitudinal translation	0.53	0.62	0.60	0.76	1.04	1.06	1.16	1.17
Global torsion	0.56	0.63	0.57	0.66	1.02	1.04	1.03	1.03
Horizontal deck deform.	0.46	0.47	0.47	0.48	0.73	0.74	0.73	0.73
Vertical deck deform.	0.40	0.41	0.41	0.46	0.52	0.52	0.52	0.53

The elongated periods of the FRC bridge, in comparison to the RC bridge, are due to increased initial flexibility incorporated in the column model, or equivalently the offset in its

elastic limit. The effectiveness of the isolation system was evident given the similarity between the pre-earthquake and post-earthquake periods obtained for the bridge systems, indicating that no significant degradation in the stiffness or strength of the nonlinear bridge model has occurred during the dynamic excitation, even for a high intensity ground motion.

Pushover Curves

The complete longitudinal and transverse pushover response of the different bridge systems, obtained by summing the shear resistance of all column bents and abutments, is presented in Figure 4. A uniform force pattern was applied on all deck nodes of the different bridge systems for comparative purposes and the displacement of the bridges was monitored at the external column top for all bridge systems. For the isolated bridges, the displacement was also monitored at the superstructure or deck level, in addition to the column top, to capture the deformation of the LRBs located between these two elements. The main pushover analysis results obtained for an external column of the different bridge systems analyzed are summarized in Table 2.

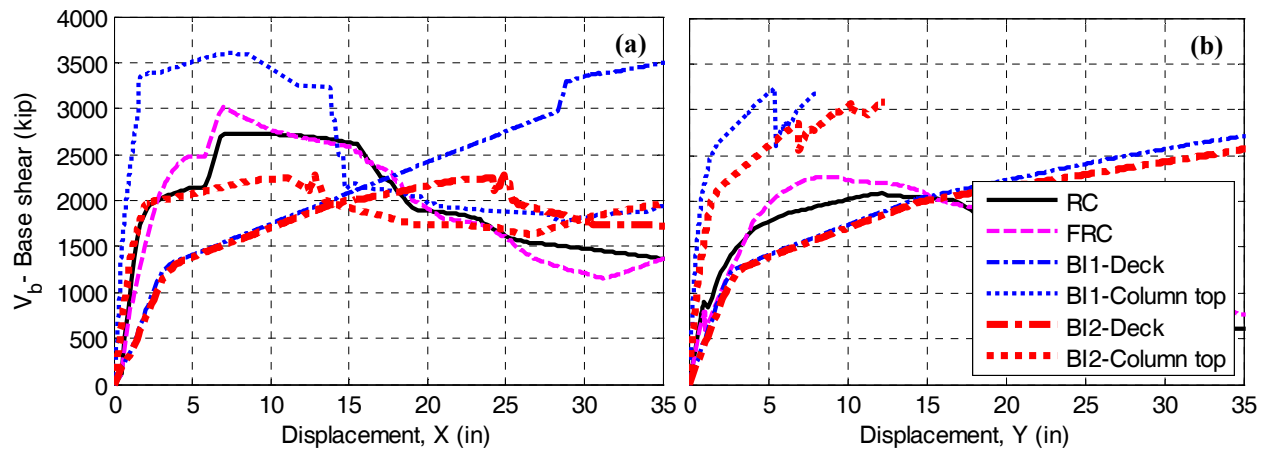


Figure 4. Pushover response for bridge systems: (a) Longitudinal; (b) Transverse.

Table 2. Longitudinal and transverse pushover analysis results for external column response.

Parameter	RC bridge	FRC bridge	BI1 bridge	BI2 bridge
$\Delta_{v,L}$, $\Delta_{v,T}$ - Long., transv. yield displ.	1.5", 2.0"	3.0", 5.0"	1.9", 1.8"	2.1", 2.1"
$V_{col,L}$, $V_{col,T}$ - Long., transv. shear	395 ^k , 387 ^k	486 ^k , 478 ^k	487 ^k , 656 ^k	306 ^k , 615 ^k
$\mu_{d,L}$, $\mu_{d,T}$ - Long., transv. displ. duct. Capacity	10.3, 8.5	5.1, 3.6	4.6, 4.5	5.2, 5.9

The overall shape of the longitudinal and transverse pushover curves of the RC and FRC bridges is similar; however, the FRC bridge model was defined with increased flexibility and resulted in increased elastic limit (yield displacement is increased by 100% and 150% in the longitudinal and transverse directions, respectively) and higher ultimate base shear capacity (approximately 10% increase in both longitudinal and transverse directions), in comparison to the RC bridge. This is due primarily to the enhanced material properties of the fiber-reinforced concrete columns obtained experimentally. Since the ultimate displacement capacity of the FRC

columns, governed primarily by the fracture strain values of the longitudinal steel reinforcement, is maintained, the displacement ductility capacity of the FRC bridge is reduced, compared to the RC bridge. However, the elastic limit of the FRC columns is significantly offset, compared to the RC bridge columns, thus delaying the initiation of permanent damage in the bridge columns. As discussed in the companion paper, despite higher force demands on the FRC bridge due to increased material strength, the enhanced damage tolerance of the fiber-reinforced concrete material and offset of its elastic limit will result in a significant reduction in the post-earthquake repair actions for the FRC bridge.

The overall shape of the pushover curves of the isolated bridges is significantly altered in comparison to the benchmark RC bridge, given a similar pushover force pattern. The initial stiffness of the isolated bridge columns is higher than the RC column due to their reduced heights and increased cross-sectional dimensions and reinforcement ratios. The increased relative flexibility of the isolated bridge superstructure results in a significant reduction in displacement and force demands on the column bents and an increased demand on the LRB isolators, for a given level of seismic intensity, especially after the LRB isolators reach their yield strength at a combined force of 200 kip. In the BI1 bridge the column flexural- and base shear capacities are significantly higher than the RC and BI2 bridges, and its elastic limit is only reached at extremely high displacement demands on the superstructure. The column flexural capacity of the BI2 bridge in the longitudinal direction is approximately 40% lower than that of the BI1 bridge. The formation of plastic hinges solely at the column base due to altered boundary conditions in the isolated bridges results in a base shear around 20% lower than the RC bridge, which forms plastic hinges at both column top and bottom, for a longitudinal pushover. The peak external column shears developed in BI1 and BI2 bridges in the transverse direction are approximately 70% and 60% higher than the RC column shear, respectively, primarily due to altered boundary conditions that result in the formation of an additional plastic hinge at the column top. Overall, the transverse response of the isolated bridges is considerably superior to the RC bridge for all demand levels. The displacement of the isolated bridges superstructure is over 30% higher than the RC bridge superstructure response until the elastic limit of the latter bridge; however, this increased flexibility and excessive deformation of the isolated bridges is produced due to stable and ductile deformation of the bearings, not the substructure or superstructure.

Nonlinear Time History Analysis Results

Nonlinear time history analysis was carried out on three-dimensional OpenSees models of the RC, FRC, and isolated bridges BI1 and BI2 by applying a uniform ground motion excitation at the base of the bridges using 140 three-component records covering a wide range of earthquake magnitudes and fault distances, as well as different faulting mechanisms. The comparison of the seismic response of the different bridge systems was carried out by relating selected EDPs obtained from nonlinear time history analysis to an intensity measure (*IM*) for each record. A natural log fit was used to relate the EDPs of the different bridges to the period-independent *IM* of each record, defined as the scaled peak ground velocity (PGV). The PGV value for each three-component ground motion, obtained as the SRSS combination of the PGV values of the two orthogonal horizontal components of the record, is an adequate *IM* for structures with fundamental first-mode period in the constant velocity range of the response spectra. The natural-log regressions on selected EDPs of the different bridge systems are

presented in Figure 5. The regressions provide an important insight on the effect of using different seismic performance enhancement techniques on the overall behavior of the bridges response parameters as a function of earthquake intensity. However, due to the high data dispersion of the nonlinear dynamic analysis results, the regressions do not provide exact relations between these parameters and earthquake intensity. A comprehensive dynamic analysis with different bridge configurations and reinforcement details, as well as an extended ground motion set, is required to compute reliable bias factors between the different bridge systems at different hazard levels.

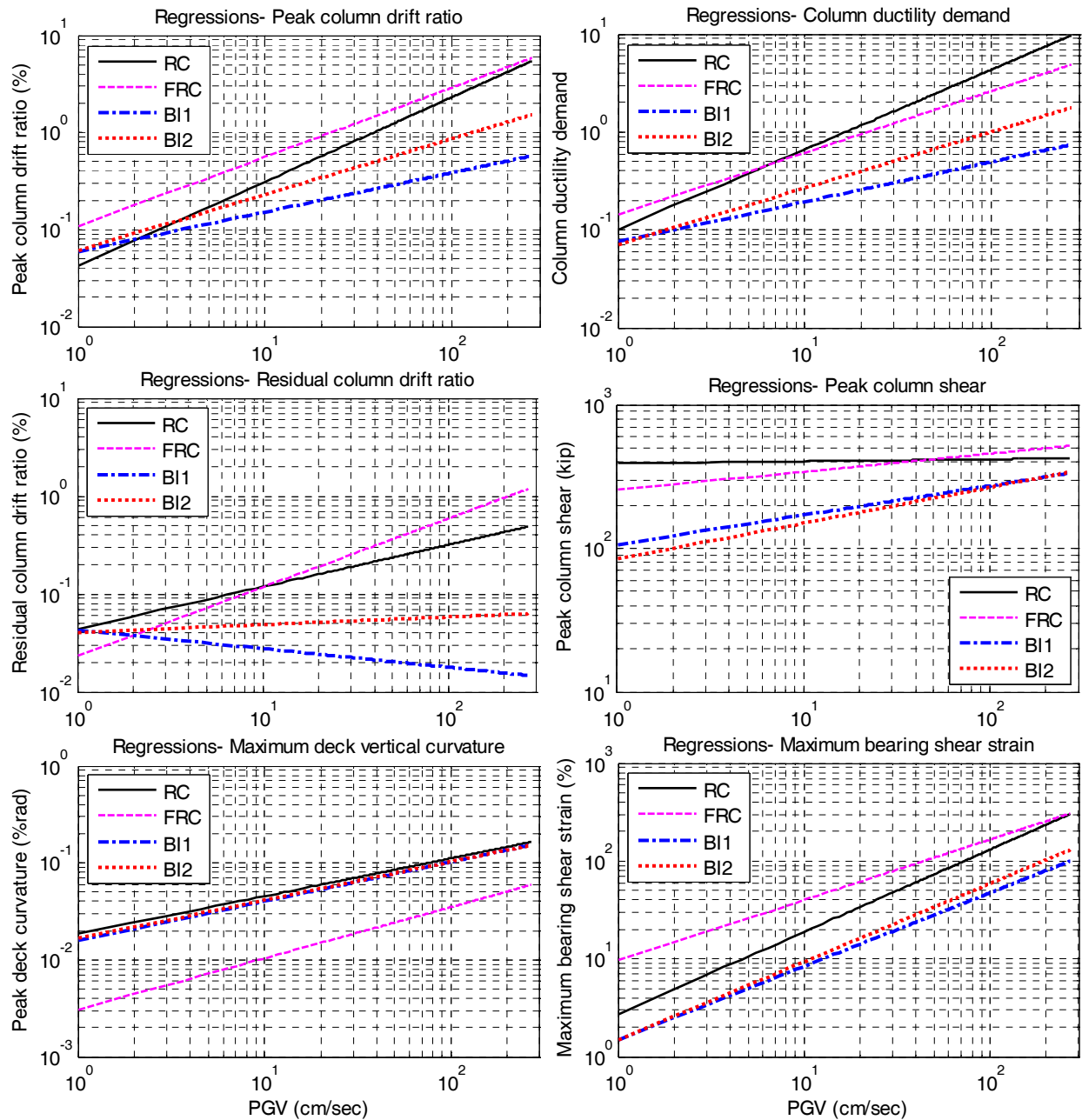


Figure 5. Natural-log regressions on important EDPs of the different bridge systems.

As seen in Figure 5, the isolation of the bridge superstructure results in a drastic reduction in the median peak drift ratio, displacement ductility, and residual drift demands, compared to the RC bridge. According to the design objectives, the reduction in deformation demand is more pronounced for the BI1 bridge column, which remains in the elastic range of response for the entire range of earthquake intensity considered, while the displacement ductility demand of the BI2 bridge column is estimated between 1 and 2 for high earthquake intensities. The design of the isolated bridges is deliberately intended to result in higher bearing displacement demands of the LRBs which provide stable hysteretic response and high energy dissipating capacity. The isolated bridges do not produce a significant effect on the peak vertical curvatures and accelerations of the superstructure, in comparison to the RC bridge; however, a significant reduction is obtained in the column shear demand for all earthquake intensities.

According to the analytical bridge results, the drift demands on the FRC present a sizeable increase, in comparison to the RC bridge, for the entire range of earthquake intensity considered. However, due to an increase in the transverse and longitudinal yield displacements of the FRC columns obtained experimentally, the resulting displacement demands on the FRC bridge column bents are in fact reduced for the medium to high earthquake intensity range. The residual drift ratio is highly sensitive to the dynamic properties of a bridge system, and in the case of the FRC bridge column, a reduction and increase in this EDP is produced for the low and high hazard levels, respectively, in comparison to the RC bridge. The analytical model of the FRC bridge results in an increase in the displacement and shear strain demand on the elastomeric bearings and a significant reduction in superstructure curvature for all seismic intensities, in comparison to the RC bridge.

Conclusions

A typical single-column bent reinforced concrete bridge in California with box-girder superstructure and no geometric irregularities was redesigned using two performance enhancement strategies: seismic isolation devices placed underneath the superstructure and high-performance fiber-reinforced concrete materials used for the construction of the bridge piers. The design of the isolated bridge included two alternative performance criteria: in one the column remained elastic for the entire range of seismic intensities considered in the study, and in the other the column was designed to undergo displacement ductility demands not greater than 2. The isolation system consisted of lead-plug rubber bearings and an additional cap beam at the column top connecting the system to the superstructure. The fiber-reinforced concrete bridge was specified with steel macro-fibers in 1.5% volume fraction, relaxed transverse reinforcement, as well as additional dowels at the column base to prevent base cracks and allow extensive propagation of the plastic hinge zone.

The assessment of the improved performance of the bridge was carried out by comparing modal, pushover, and nonlinear time history analyses results of detailed nonlinear three-dimensional models of these bridge systems implemented in OpenSees. In general, both base isolated and the fiber-reinforced concrete bridge behaved better than the reference reinforced concrete bridge. The fiber-reinforced concrete bridge has a higher elastic limit and base shear capacity than the benchmark bridge, resulting in reduced displacement ductility demands, as well as increased bearing displacement and shear strain demands which are easily compensated for by the enhanced shear and flexural strength, as well as improved damage tolerance. For the isolated bridges, the location of the bearings at the column top reduced column heights, subsequently

requiring larger and more reinforced columns resulted in an increased stiffness and reduced ductility capacity of the column bents; however this was not relevant since the isolated columns only undergo minor ductility demands even at high seismic intensity levels. The isolation system design was highly effective in reducing displacement demands (maximum drift, displacement ductility, and residual drift), as well as shear demands on the substructure. The inelastic response and energy dissipation in both isolated bridges was developed solely through the stable and ductile post-yield shear deformation of the isolator devices.

References

- Aoude, H., Cook, W.D., and Mitchell, D., 2009. Behavior of Columns Constructed with Fibers and Self-Consolidating Concrete, *ACI Structural Journal*, 106(3), 349-357.
- Aviram, A., Mackie, K., and Stojadinovic, B., 2008. Effect of Abutment Modeling on the Seismic Response of Bridge Structures, *Proceedings of the 6th National Seismic Conference on Bridges and Highways*, Charleston, South Carolina.
- Aviram, A., Mackie, K. and Stojadinovic, B., 2008. Guidelines for Nonlinear Analysis of Bridge Structures in California, *Technical Report 2008/03, Pacific Earthquake Engineering Research Center*, University of California, Berkeley.
- Billington, S.L. and Yoon, J.K., 2004. Cyclic Response of Precast Bridge Columns with Ductile Fiber-reinforced Concrete, *ASCE Journal of Bridge Engineering*. 9(4), 353-363.
- Buckle, I.G., Constantinou, M.C., Dicleli, M., and Ghasemi, H., 2006. Seismic Isolation of Highway Bridges, *Special Publication MCEER-06-SP07*, Multidisciplinary Center for Extreme Events Research, Buffalo, New York.
- Filiatrault, A., Pineau, S., and Houde, J., 1995. Seismic Behavior of Steel-Fiber Reinforced Concrete Interior Beam-Column Joints, *ACI Structural Journal*, 92(5), 1-10.
- Grant, D., Fenves, G.L., and Auricchio, F., 2004. Bridge isolation with high-damping rubber bearings-analytical modelling and system response, *Proceedings of the 13th World Conference on Earthquake Engineering*, Vancouver, B.C.
- Kelly, J.M., 1997. *Earthquake-Resistant Design with Rubber*, 2nd Edition, Springer Verlag.
- Ketchum, M., Chang, V., and Shantz, T., 2004. *Influence of Design Ground Motion Level on Highway Bridge Costs*, Report No. Lifelines 6D01, University of California, Pacific Earthquake Engineering Research Center, Berkeley, California.
- Lee, W., Jeong, H., Billington, S., Mahin, S.A., and Sakai, J., 2007. Post-Tensioned Structural Concrete Bridge Piers with Self-Centering Characteristics, *Proceedings of the 2007 Structures Congress*, Long Beach, California.
- Mckenna, F., Fenves, G.L., Scott, M.H., and Jeremic, B., 2000. *Open system for earthquake engineering simulation*, <http://opensees.berkeley.edu>.
- Mosqueda, G., Whittaker, A., Fenves, G.L., and Mahin, S.A., 2004. Experimental and analytical studies of the friction pendulum system for the seismic protection of simple bridges, *Report UCB/EERC-2004/01*, Earthquake Engineering Research Center, University of California, Berkeley.
- Naaman, A.E., Likhitrungslip, V., and Parra-Montesinos, G., 2007. Punching Shear Response of High-Performance Fiber-Reinforced Cementitious Composite Slab, *ACI Structural Journal*, 140(2), 170-179.
- Saiidi, S.M., O'Brien, M., and Sadrossadat-Zadeh, M., 2009. Cyclic Response of Concrete Bridge Columns Using Superelastic Nitinol and Bendable Concrete, *ACI Structural Journal*, 106(1), 69-77.
- Warn, G.P., and Whittaker, A.S. 2004. Performance Estimates in Seismically Isolated Bridge Structures, *Engineering Structures*, 26(9), 1261-1278.